Ionization, Single and Double Electron Capture in Proton-Ar Collisions

A. Jorge,[†,‡] Clara Illescas,[†] L. Méndez,[*,†] and I. Rabadán[†]

†*Laboratorio Asociado al CIEMAT de Física Atómica y Molecular en Plasmas de Fusión. Departamento de Química, módulo 13, Universidad Autónoma de Madrid, 28049-Madrid, Spain.*

‡*Current address: Department of Physics and Astronomy, York University, Toronto, Ontario, M3J 1P3, Canada*

E-mail: l.mendez@uam.es

Abstract

Total cross sections for formation of H and H^-, and electron production, in H^++Ar collisions have been calculated at energies between 100 eV and 200 keV employing two methods: for $E < 10$ keV, a semiclassical treatment with an expansion in a basis of electronic wave functions of the ArH^+ quasimolecule and, for $E > 10$ keV, the switching-Classical-Trajectory-Monte-Carlo method (s-CTMC). The semiclassical calculation involves transitions to molecular autoionizing states, calculated by applying a block-diagonalization technique. The s-CTMC method is adept to treat two-electron processes and yields total cross sections for H^- formation in reasonably good agreement with the experimental data. Cross sections for electron- and H-production processes, which are dominated by one-electron transitions, are in good agreement with the experimental data.

1. Introduction

Negative ions play a significant role in astrophysics (see e.g. Refs. 1,2); specifically, the formation of H_2 in first protogalaxies takes place by associative detachment in collisions of H^- with H.[3] Anions are also important in the chemistry of planetary atmospheres[4] and in low-temperature plasmas.[5] The efficient production of H is a critical issue in the design of neutral beam injection systems of fusion devices (Ref. 6 and references therein). Negative ions are also formed in ion or photon interaction with living tissue that takes place in cancer therapy, which has motivated the study of anion-molecule collisions.[7,8] The formation of negative ions in collisions of positive ions with atoms and molecules has been studied in several works.[9–23] In particular, collisions of protons with atoms can lead to the formation of H^- via two-electron capture, but even for these relatively simple atomic systems the theoretical description of H^- formation is difficult since the double capture probability is two orders of magnitude smaller than those of one-electron processes like single electron capture or single ionization.[10–14,17,21,23]

In this paper we consider proton–argon collisions at energies between 0.1 and 200 keV. At $E < 25$ keV, the most important process is the single-electron capture (SC)

$$H^+ + Ar \rightarrow H + Ar^+. \tag{1}$$

The single ionization (SI):

$$H^+ + Ar \rightarrow H^+ + Ar^+ + e, \tag{2}$$

which involves the removal of one-electron from the target, becomes dominant at $E > 25$ keV. Two-electron processes also take place, and specifically H^- can be produced in the double-electron-capture (DC) reaction:

$$H^+ + Ar \rightarrow H^- + Ar^{2+}. \tag{3}$$

Cross sections for production of H have been measured in Refs. 24–32, where H is formed in the SC reaction (1), but also via the transfer ionization (TI) process

$$H^+ + Ar \rightarrow H + Ar^{2+} + e\ . \tag{4}$$

The total cross section for production of H^- was measured in several experiments;[9–11,13,17] this anion is formed in the DC reaction, but also in three-electron processes such as

$$H^+ + Ar \rightarrow H^- + Ar^{3+} + e, \tag{5}$$

which is expected to be less relevant than (3). Ar^{2+} can also be formed in the double ionization (DI) process:

$$H^+ + Ar \rightarrow H^+ + Ar^{2+} + 2e. \tag{6}$$

Total cross sections for formation of Ar^{q+} were measured by Dubois et al.[33] The experiments show that the total cross section for formation of H^- is about two orders of magnitude smaller

than those of the SC and SI reactions and it exhibits two maxima at $E \approx 5$ and 25 keV. Differential cross sections for production of H^- in the energy range $1 \leq E \leq 5$ keV were measured by Martinez et al.[17]

H^++Ar collisions were studied theoretically by Kirchner and coworkers[34–36] employing a one-electron method with a target model potential that includes dynamical screening effects; the ensuing one-electron time-dependent Schrödinger equation was solved by using the so-called Basis Generator method (BGM). The application of the Independent Particle Model (IPM) yielded cross sections for q-fold electron-loss. They found general good agreement with the experiments for net ionization and electron capture for $E \gtrsim 10$ keV. However, this method, which does not include explicitly the electron-electron interaction, cannot accurately calculate the cross section for DC. Amaya-Tapia et al.[37] calculated SC total and partial cross sections by employing a one-electron wavefunction expanded in a basis set of atomic orbital with the IPM (CCAO-IPM). Martinez et al.[17] calculated the DC total cross section by applying a two-center atomic basis set. Cabrera-Trujillo et al.[38] applied the electron-nuclear dynamics (END) method and a CCAO-IPM treatment to calculate differential and total cross sections for SC. More recently, Wang et al.[21] have calculated total cross sections for reactions (1) and (3) by applying a time-dependent-density-functional model. Their results for SC agree with the experiments in a wide energy range $1 < E < 400$ keV, but the calculated DC cross sections overestimate the experimental ones by about one order of magnitude. Fremont[23] has employed the Classical Trajectory Monte Carlo (CTMC)[39] with the active electron moving in a model potential. The calculated SC cross section agree with the experiments, but the use of the IPM leads to the overestimation of the DC total cross section. Juháshz[40] has developed a statistical model to estimate differential cross sections for H^- production that has been applied to production of H^- in several systems and in particular to DC in H^++Ar collisions.

In this paper we carry out a theoretical study of H^++Ar collisions by applying two methods. We apply a semiclassical method with a close-coupling expansion in terms of many-

electron molecular wave functions (MFCC) with eight active electrons, and the switching Classical Trajectory Monte Carlo (s-CTMC) method, recently proposed by Jorge et al.[41] In the classical calculations we have considered the motion of two electrons in a model potential. Both methods employ effective potentials to describe the $n = 1 - 2$ shells that do not play a significant role at energies below 500 keV, as indicated by the negligible contribution of Auger electron emission.[42,43] One can note that the use of effective potentials for two-electron collisions was already considered in the pioneering works of Mó et al.[44,45] and Errea et al.[46]

The expansion in terms of molecular functions (see, e.g. 47) has been widely applied to collisions at low energies, but it presents important limitations at collision energies above a few keV/u (see Errea et al.[48] and references therein), where the ionizing processes are competitive with the electron-capture reactions. Since the expansion in terms of L^2 integrable functions cannot describe the transitions to the electronic continuum, the electronic flux that should yield ionization remains in the molecular states that correlate to the electron capture channels, which in practice are overpopulated, and the SC cross section is overestimated. It is found that the molecular expansion provides the electron-loss cross section (the sum of ionization and capture cross sections) when the ionization starts to be significant. On the other hand, since the MFCC method employs many-electron functions, it does not require to employ the IPM approximation. For the particular case of H^++Ar collisions, the calculation of SC cross sections involves only a few molecular states; however, the DC process occurs through transitions to infinitely excited states, which lie in the continuum above one Rydberg series. The description of the DC reaction is carried out by using a block-diagonalization (BD) technique to calculate the potential energy curves (PECs) of the molecular states that lie above the ionization threshold.

The s-CTMC is based on the CTMC[39] method, where the electron motion is described by a classical distribution, and it has been successfully applied to calculate ionization and capture cross sections for collisions in one-electron systems.[49] Nevertheless, the extension of the CTMC method to many-electron systems is not straightforward because a classical

two- (or many-) electron system is unstable. It is well-known that the electron-electron repulsion term is responsible for the unphysical autoionization of the classical He atom, where one electron loses energy moving to a trajectory with smaller radius and the other electron is ejected. In order to circumvent this limitation, the s-CTMC method describes a two-electron collision system by means of the two-electron hamiltonian, including the electron-electron repulsion term, when the electrons are bound to different nuclei and the unphysical autoionization does not take place. However, when both electrons are bound to the same nucleus, a model-potential description is applied for both electrons. The method has been successfully applied H+H and H^++H^- collisions,[41] yielding total cross sections in good agreement with the experimental ones. The present work is the extension of the method to systems with several electron pairs.

The paper is organized as follows. In section 2 we summarize the methods, MFCC and s-CTMC, employed in our calculations. The calculated PECs of the ArH^+ quasimolecule are presented in section 3.1, where we discuss the application of the BD method. We present in section 3.2 the dynamical results of the application of the MFCC method, and in sections 3.3 and 3.4 the results of the s-CTMC calculation. Our results are summarized in section 4. Atomic units are employed unless otherwise stated.

2. Theoretical methods.

2.1 Semiclassical MFCC method

In the semiclassical calculation we employ the impact parameter approximation in which the nuclei follow straight-line trajectories $\boldsymbol{R} = \boldsymbol{b} + \boldsymbol{v}t$, where $\boldsymbol{R}$ is the internuclear vector, $\boldsymbol{b}$ the impact parameter vector, and $\boldsymbol{v}$ the relative velocity. The electronic degrees of freedom are described quantum-mechanically by the wave function $\Psi(\boldsymbol{r}, t; b, v)$, where $\boldsymbol{r}$ is the set of

electron coordinates. Ψ is a solution of the semiclassical equation:

$$H_{\rm el}\Psi = i\frac{\partial\Psi}{\partial t}, \tag{7}$$

where $H_{\rm el}$ is the clamped-nuclei Born-Oppenheimer electronic hamiltonian. We apply an effective potential approach that assumes that the valence electrons move in the average potential created by nucleus and the core electrons. Accordingly $H_{\rm el}$ for H^++Ar collisions has the form:

$$H_{\rm el}(\boldsymbol{r};R) = \sum_{i=1}^{N_{\rm el}}\left[-\frac{\nabla_i^2}{2} + V^{\rm sp}(r_i) - \frac{Z_{\rm H}}{r_{{\rm H}i}}\right] + \sum_{i>j}^{N_{\rm el}}\frac{1}{r_{ij}} + \frac{Z_{\rm Ar}Z_{\rm H}}{R} \tag{8}$$

In this expression, $Z_{\rm Ar} = 18$ and $Z_{\rm H} = 1$ are the nuclear charges and $N_{\rm el} = 8$ the number of active electrons electrons; $\boldsymbol{r}_i$ are the electron position vectors with respect to the Ar nucleus and $\boldsymbol{r}_{{\rm H}i}$ are the electron position vectors with respect to the H nucleus. $V^{\rm sp}(r_i)$ is a pseudopotential. In the calculations we have employed the relativistic pseudopotential of Pacios and Christiansen.[50]

The collision wave function is expanded in a set of molecular functions, $\phi_k(\boldsymbol{r};R)$ which are approximate eigenfunctions of $H_{\rm el}$:

$$\Psi(\boldsymbol{r},t;b,v) = D(\boldsymbol{r},t)\sum_k a_k(t;b,v)\phi_k(\boldsymbol{r};R)\exp\left[-i\int_0^t {\rm d}t\varepsilon_k(R)\right], \tag{9}$$

where D is a common translation factor[51] and ε_k are the electronic energies that are the approximate eigenvalues of $H_{\rm el}$

$$H_{\rm el}(\boldsymbol{r};R)\phi_k(\boldsymbol{r};R) = \varepsilon_k(R)\phi_k(\boldsymbol{r};R). \tag{10}$$

The substitution of the expansion (9) into the semiclassical equation (7) leads to a set of first-order differential equations for the coefficients $a_k(t)$. If the system is initially described

by the molecular function ϕ_i, the system of differential equations is solved with the initial condition

$$\lim_{t\to-\infty} a_k(t) = \delta_{ik}. \tag{11}$$

The transitions are driven by the non-adiabatic (also called dynamical) couplings, which are proportional to the matrix elements of the nuclear gradient. The probability, $P_j(b, E)$ for the transition from ϕ_i to ϕ_j is:

$$P_j(b, E) = \lim_{t\to+\infty} |a_j(t) - \delta_{ij}|^2, \tag{12}$$

and the total cross section for this transition is:

$$\sigma_j(E) = 2\pi \int_0^\infty b P_j(b, E). \tag{13}$$

The differential cross section can be calculated, in the impact parameter approximation, from the coefficient a_k, as explained by Piacentini and Salin.[52] However, in this work we have employed the simple expression:[53,54]

$$\frac{d\sigma_j(\theta, E)}{d\Omega} = \left[\frac{d\sigma(\theta)}{d\Omega}\right]_{\text{classical}} P_j(b, E), \tag{14}$$

which is obtained[53] by applying the stationary phase approximation to the partial wave expression of the differential cross section, and the substitution of the stationary phase momentum by the classical momentum that corresponds to the classical scattering angle. In the simple formula (14), the inelastic differential cross section is given by the product of the elastic classical differential cross section and the semiclassical transition probability. The application of this expression requires the correspondence between the scattering angle (in the laboratory frame) and the impact parameter. Previous work for He^{2+}+H collisions of Winter et al.[55] used this expression with Coulomb trajectories. They found that the results for electron-capture cross sections agreed with those obtained without using the stationary

phase approximation with about 10–20% errors for energies between 1 and 70 keV. The equation (14) was also employed by Errea et al.[56] to discuss the shape of the elastic cross section in He^++H collisions for $1.5 < E < 5$ keV. This latter work pointed out that, the use of Coulomb trajectories, defined by the nuclear repulsion interaction, yields results that agree with those obtained from the use of the energy of the entrance channels for $E \geq 10$ keV, which is more accurate at lower energies. Since we have applied the approximation (14) at $1 < E < 5$ keV, we have calculated the classical deflection function and the ensuing differential cross section with the energy $\varepsilon_1(R)$ of the ground electronic state of ArH^+.

2.2 s-CTMC method

As in the semiclassical method of subsection 2.1, we assume in the CTMC calculations rectilinear nuclear trajectories.[57] For a one-electron system, the electronic motion is represented, for each nuclear trajectory, by a classical distribution function $\rho(\boldsymbol{r}, \boldsymbol{p}, t; b, E)$, where $\boldsymbol{r}$ and $\boldsymbol{p}$ are, respectively, the electron position and momentum vectors. The electron distribution is a solution of the Liouville equation:

$$\frac{\partial \rho}{\partial t} = -[\rho, H], \tag{15}$$

where $H(\boldsymbol{r}, \boldsymbol{p}, t)$ is the classical hamiltonian for the electron motion. The discretization of the distribution leads to the Hamilton equations that define a set of N electron trajectories $\{\boldsymbol{r}_k(t), \boldsymbol{p}_k(t)\}_{k=1,\ldots,N}$. In the present application, we consider two independent electrons that are initially bound to the Ar atom. The interaction of the active electrons with the Ar^+ core is described by the central model potential:[58]

$$V_{Ar^+}(r) = -\frac{Z - N_c}{r} - \frac{Ae^{-Br} + (N_c - A)e^{-Cr}}{r} \tag{16}$$

With $Z = 18, N_c = 17$; the parameters $A = 5.4, B = 1, C = 3.682$ have been obtained by fitting the Ar ionization energies.[59] This model potential has been previously employed in

CTMC calculations by Labaigt et al.[60] The total classical hamiltonian for each electron pair is:

$$H(\boldsymbol{r}_1, \boldsymbol{r}_2, \boldsymbol{p}_1, \boldsymbol{p}_2, t) = h(\boldsymbol{r}_1, \boldsymbol{p}_1, t) + h(\boldsymbol{r}_2, \boldsymbol{p}_2, t), \tag{17}$$

with

$$h(\boldsymbol{r}_i, \boldsymbol{p_i}, t) = \frac{p_i^2}{2} + V_{\mathrm{Ar}^+}(r_i) - \frac{1}{r_{\mathrm{H}i}}. \tag{18}$$

Initially, both electrons are bound to the Ar nucleus and we have:

$$h(\boldsymbol{r}_i, \boldsymbol{p_i}, t \to -\infty) = h^{\mathrm{ini}}(\boldsymbol{r}_i, \boldsymbol{p_i}) = \frac{p_i^2}{2} + V_{\mathrm{Ar}^+}(r_i), \tag{19}$$

and the system is described by products of two independent microcanonical distributions:

$$\rho(\boldsymbol{r}_1, \boldsymbol{r}_2, \boldsymbol{p}_1, \boldsymbol{p}_2, t \to -\infty; b, v) = K^{-1}\delta[h^{\mathrm{ini}}(\boldsymbol{r}_1, \boldsymbol{p}_1) - \epsilon^l_{\mathrm{Ar}}]\delta[h^{\mathrm{ini}}(\boldsymbol{r}_2, \boldsymbol{p}_2) - \epsilon^l_{\mathrm{Ar}}], \tag{20}$$

where K^{-1} is a normalization constant and ϵ^l_{Ar} (with $l = 0, 1$) are, respectively, the energies of the orbitals $3s$ and $3p$. The distributions have been generated as explained in Ref. 61. When the collision starts, the two electrons remain bound to the Ar nucleus and the two one-electron hamiltonians,

$$h_{\mathrm{Ar}}(\boldsymbol{r}_i, \boldsymbol{p}_i, t) = \frac{p_i^2}{2} + V_{\mathrm{Ar}^+} \quad \text{with } i = 1, 2, \tag{21}$$

are negative, while the corresponding ones with respect to the H reference frame,

$$h_{\mathrm{H}}(\boldsymbol{r}_i, \boldsymbol{p}_i, t) = \frac{(p_i - v)^2}{2} - \frac{1}{r_{\mathrm{H}i}} \quad \text{with } i = 1, 2, \tag{22}$$

are positive.

During the collision, the electron i can be captured, yielding $h_{\mathrm{Ar}}(\boldsymbol{r}_i, \boldsymbol{p}_i, t) > 0$ and $h_{\mathrm{H}}(\boldsymbol{r}_i, \boldsymbol{p}_i, t) < 0$. In this case, each electron is bound to different nuclei and the classical two-electron system is stable. Therefore, the electron-electron repulsion is explicitly

included, and then we switch to the hamiltonian:

$$H = \frac{p_1^2}{2} + \frac{p_2^2}{2} + V_{\mathrm{Ar}^{2+}}(r_1) + V_{\mathrm{Ar}^{2+}}(r_2) - \frac{1}{r_{\mathrm{H}_1}} - \frac{1}{r_{\mathrm{H}_2}} + \frac{1}{r_{12}} \tag{23}$$

The new hamiltonian includes a model potential $V_{\mathrm{Ar}^{2+}}$ to describe the electron interaction with the Ar^{2+} core. This model potential is of the form of Eq. (16) and with $Z = 18, N = 16, A = 7.704, B = 5.796, C = 1.413$, obtained using the Talman's code.[62]

If both electrons are captured, the classical system is unstable when including the electron-electron repulsion term. Accordingly, we switch to the model-potential description, as in Jorge et al.[41]

$$H(\boldsymbol{r}_1, \boldsymbol{r}_2, \boldsymbol{p}_1, \boldsymbol{p}_2, t) = h(\boldsymbol{r}_1, \boldsymbol{p}_1, t) + h(\boldsymbol{r}_2, \boldsymbol{p}_2, t), \tag{24}$$

where

$$h(\boldsymbol{r}_i, \boldsymbol{p_i}, t) = \frac{p_i^2}{2} + V_{\mathrm{H}}(r_i) + V_{\mathrm{Ar}^{2+}}(r_i) \tag{25}$$

and

$$V_{\mathrm{H}}(r_i) = -\frac{1 + \alpha r_{\mathrm{H}i}}{r_{\mathrm{H}i}} \exp\left(-2\alpha r_{\mathrm{H}i}\right) \tag{26}$$

with $\alpha = 0.65$ (see Ref. 41). In this case, we have for both electrons:

$$\epsilon_{\mathrm{Ar}}(i) = \frac{p_i^2}{2} + V_{\mathrm{Ar}^{2+}}(r_i) > 0 \quad \text{(Ar reference frame)} \tag{27}$$

$$\epsilon_{\mathrm{H}}(i) = \frac{(p_i - v)^2}{2} + V_{\mathrm{H}}(|\boldsymbol{r}_i - \boldsymbol{R}|) < 0 \quad \text{(H reference frame)} \tag{28}$$

In the limit $t \to \infty$, the trajectories are classified according to the electronic energies of both electrons in the two reference frames $\epsilon_{\mathrm{Ar}}(i)$ and $\epsilon_{\mathrm{H}}(i)$:

- Elastic collision or electronic excitation (E): $\epsilon_{\mathrm{Ar}}(1) < 0$ and $\epsilon_{\mathrm{Ar}}(2) < 0$.
- Single electron capture (SC): $\epsilon_{\mathrm{Ar}}(i) < 0$ and $\epsilon_{\mathrm{H}}(j) < 0$.
- Single ionization (SI): $\epsilon_{\mathrm{Ar}}(i) < 0$ and both $\epsilon_{\mathrm{Ar}}(j) > 0$ $\epsilon_{\mathrm{H}}(j) > 0$.

- Transfer ionization (TI): $\epsilon_{\rm H}(i) < 0$ and both $\epsilon_{\rm Ar}(j) > 0$ $\epsilon_{\rm H}(j) > 0$.
- Double ionization (DI): $\epsilon_{\rm Ar}(i) > 0$ and $\epsilon_{\rm H}(i) > 0$ for both electrons.
- Double electron capture (DC): $\epsilon_{\rm H}(i) < 0$ for both electrons with $\epsilon_{\rm Ar}(i) > 0$ for both electrons.

In the calculations, the two-electron trajectories are integrated from an initial nuclei position $Z_{\rm in} = vt_{\rm in}$ up to $Z_{\rm f} = vt_{\rm f}$ (in our calculation $Z_{\rm in} = -50$ bohr; $Z_{\rm f} = 500$ bohr), and the probability of each process, for a given collision with impact parameter b and energy E, $p_{\rm r}(b, E)$, is the fraction of trajectories yielding this particular process:

$$p_{\rm r}(b, E) = \frac{N_{\rm r}}{N}\,, \quad \text{with r=E, SC, SI, TI, DI, DC.} \tag{29}$$

In the present calculation we have employed $N = 10^6$ trajectories for $E \leq 100$ keV and $N = 4.84 \times 10^6$ trajectories for $E > 100$ keV, where the calculation of small probabilities requires a larger statistics.

For a given electron pair, the probabilities fulfill:

$$1 = p_{\rm E} + p_{\rm SC} + p_{\rm SI} + p_{\rm TI} + p_{\rm DI} + p_{\rm DC}\,. \tag{30}$$

Assuming that the four valence electron pairs are independent, we can obtain the probabilities, $P_{\rm r}$ for the eight-electron system from the corresponding two electron probabilities of (29). Explicitly, if we call $p_{\rm r}^{ss}$ the probabilities for the process r starting from a pair of electrons in the $3s$ orbital, $p_{\rm r}^{mm}$ the corresponding probability for a pair of electrons in the $3p$ orbital with a value m of the magnetic quantum number, we can express the probability for H formation in the form:

$$P_{\rm H} = (p_{\rm SC}^{ss} + p_{\rm TI}^{ss}) \prod_{m_i} (1 - p_{\rm SC}^{m_i m_i} - p_{\rm TI}^{m_i m_i} - p_{\rm DC}^{m_i m_i}) +$$
$$\sum_{m_i} (p_{\rm SC}^{m_i m_i} + p_{\rm TI}^{m_i m_i}) (1 - p_{\rm SC}^{ss} - p_{\rm TI}^{ss} - p_{\rm DC}^{ss}) \prod_{m_j \neq m_i} \left(1 - p_{\rm SC}^{m_j m_j} - p_{\rm TI}^{m_j m_j} - p_{\rm DC}^{m_j m_j}\right). \tag{31}$$

This expression corresponds to an inclusive probability, where one electron is captured but the other electrons can be ionized. Likewise, using $p_{\rm E}$, an exclusive probability for SC can be defined, in which the other electrons are neither captured nor released:

$$P_{\rm SC} = p_{\rm SC}^{ss} \prod_{m_i} p_{\rm E}^{m_i m_i} + \sum_{m_i} p_{\rm SC}^{m_i m_i} p_{\rm E}^{ss} \prod_{m_j \neq m_i} p_{\rm E}^{m_j m_j}, \tag{32}$$

but there are not an experimental counterpart of this expression.

The calculations have been carried out by including in the initial distribution (20) for the $3p$ orbital trajectories with all possible values of ℓ_z. This distribution is an average of the three initial distributions considered in (31). Substituting the pair-electron probabilities by the corresponding values from the average distribution ($p_{\rm r}^{m_i m_i} = p_{\rm r}^{pp}$), one obtains:

$$P_{\rm H}^{\rm IP2} = \left(p_{\rm SC}^{ss} + p_{\rm TI}^{ss}\right) \left(1 - p_{\rm SC}^{pp} - p_{\rm TI}^{pp} - p_{\rm DC}^{pp}\right)^3 + 3 \left(p_{\rm SC}^{pp} + p_{\rm TI}^{pp}\right) \left(1 - p_{\rm SC}^{ss} - p_{\rm TI}^{ss} - p_{\rm DC}^{ss}\right) \left(1 - p_{\rm SC}^{pp} - p_{\rm TI}^{pp} - p_{\rm DC}^{pp}\right)^2 . \tag{33}$$

This formula yields the inclusive SC probability within the independent-pair treatment (IP2). As in the standard IPM treatment, it considers that the one-electron exchange from the $3s$ orbital, first term of (33), does not modify the probabilities for one-electron removal from the $3p$ subshell. Nevertheless, it can be argued that the removal of the second electron takes place from an orbital of the cation Ar^+ with a significantly smaller probability. Similarly, in the second term of (33), the probabilities for the removal of the $3s$ electrons are not modified by the exchange from the $3p$ subshell. This is the basis of the so-called independent event model (IEVM).[63] In previous calculations[64,65] for ion-H_2O collisions, we have applied this approach by neglecting the probabilities for the removal of the second electron from a different subshell, which leads to:

$$P_{\rm H}^{\rm IEV} = \left(p_{\rm SC}^{ss} + p_{\rm TI}^{ss}\right) + 3 \left(p_{\rm SC}^{pp} + p_{\rm TI}^{pp}\right) \left(1 - p_{\rm SC}^{pp} - p_{\rm TI}^{pp} - p_{\rm DC}^{pp}\right)^2 . \tag{34}$$

The double-capture process can take place by the capture of electrons either from the same orbital or from two different orbitals. The DC from the same orbital is:

$$P_{\rm DC}^{(1)} = p_{\rm DC}^{ss} \prod_{m_i} \left(1 - p_{\rm SC}^{m_i m_i} - p_{\rm TI}^{m_i m_i} - p_{\rm DC}^{m_i m_i}\right) + \sum_{m_i} p_{\rm DC}^{m_i m_i} \left(1 - p_{\rm SC}^{ss} - p_{\rm TI}^{ss} - p_{\rm DC}^{ss}\right) \prod_{m_j \neq m_i} \left(1 - p_{\rm SC}^{m_j m_j} - p_{\rm TI}^{m_j m_j} - p_{\rm DC}^{m_j m_j}\right). \quad (35)$$

The DC from two p orbitals is:

$$P_{\rm DC}^{(2)} = \sum_{m_i} \sum_{m_j < m_i} p_{\rm DC}^{m_i m_j} \left(1 - p_{\rm SC}^{ss} - p_{\rm TI}^{ss} - p_{\rm DC}^{ss}\right) \left(1 - p_{\rm SC}^{m_i m_k} - p_{\rm TI}^{m_i m_k} - p_{\rm DC}^{m_i m_k}\right) \left(1 - p_{\rm SC}^{m_j m_k} - p_{\rm TI}^{m_j m_k} - p_{\rm DC}^{m_j m_k}\right) (k \neq i \text{ and } k \neq j). \quad (36)$$

Finally, it is possible to capture one electron from the $3s$ and one electron from the $3p$ orbital, which leads to:

$$P_{\rm DC}^{(3)} = \sum_{m_i} p_{\rm DC}^{s m_i} \left(1 - p_{\rm SC}^{s m_i} - p_{\rm TI}^{s m_i} - p_{\rm DC}^{s m_i}\right) \prod_{m_j \neq m_i} \left(1 - p_{\rm SC}^{m_j m_j} - p_{\rm TI}^{m_j m_j} - p_{\rm DC}^{m_j m_j}\right). \quad (37)$$

In order to evaluate the probabilities $P_{\rm r}^{s m_i}$, we have calculated the transition probabilities with an initial distribution of the form:

$$\rho(\boldsymbol{r}_1, \boldsymbol{r}_2, \boldsymbol{p}_1, \boldsymbol{p}_2, t \to -\infty; b, v) = K^{-1} \delta[h^{\rm ini}(\boldsymbol{r}_1, \boldsymbol{R}) - \epsilon_{\rm Ar}^{s}] \delta[h^{\rm ini}(\boldsymbol{r}_2, \boldsymbol{R}) - \epsilon_{\rm Ar}^{p}] \quad (38)$$

As in (33) and (41), we have employed in the calculations of the DC probability a single p distribution that includes all projections of the angular momentum on the Z axis, which yields the approximate expression:

$$P_{\rm DC}^{\rm IP2} = p_{\rm DC}^{ss} \left(1 - p_{\rm SC}^{pp} - p_{\rm TI}^{pp} - p_{\rm DC}^{pp}\right)^3 + 6 p_{\rm DC}^{pp} \left(1 - p_{\rm SC}^{ss} - p_{\rm TI}^{ss} - p_{\rm DC}^{ss}\right) \left(1 - p_{\rm SC}^{pp} - p_{\rm TI}^{pp} - p_{\rm DC}^{pp}\right)^2 + 3 p_{\rm DC}^{sp} \left(1 - p_{\rm SC}^{sp} - p_{\rm TI}^{sp} - p_{\rm DC}^{sp}\right) \left(1 - p_{\rm SC}^{pp} - p_{\rm TI}^{pp} - p_{\rm DC}^{pp}\right)^2. \quad (39)$$

The IEVM version of this formula has the form:

$$P_{\rm DC}^{\rm IEV} = p_{\rm DC}^{ss} + 6p_{\rm DC}^{pp}\left(1 - p_{\rm SC}^{pp} - p_{\rm TI}^{pp} - p_{\rm DC}^{pp}\right)^2 + 3p_{\rm DC}^{sp}\left(1 - p_{\rm SC}^{sp} - p_{\rm TI}^{sp} - p_{\rm DC}^{sp}\right). \tag{40}$$

Using this formalism, one can also evaluate the inclusive probability $P_{\rm 1ee}^{\rm IP2}$ for the one-electron emission process, in which the single ionization takes place either without electron transfer or together with one- or two-electron transfer:

$$P_{\rm 1ee}^{\rm IP2} = \left(p_{\rm SI}^{ss} + p_{\rm TI}^{ss}\right)\left(1 - p_{\rm SI}^{pp} - p_{\rm TI}^{pp} - p_{\rm DI}^{pp}\right)^3 + 3\left(p_{\rm SI}^{pp} + p_{\rm TI}^{pp}\right)\left(1 - p_{\rm SI}^{ss} - p_{\rm TI}^{ss} - p_{\rm DI}^{ss}\right)\left(1 - p_{\rm SI}^{pp} - p_{\rm TI}^{pp} - p_{\rm DI}^{pp}\right)^2. \tag{41}$$

and in the IEVM:

$$P_{\rm 1ee}^{\rm IEV} = \left(p_{\rm SI}^{ss} + p_{\rm TI}^{ss}\right) + 3\left(p_{\rm SI}^{pp} + p_{\rm TI}^{pp}\right)\left(1 - p_{\rm SI}^{pp} - p_{\rm TI}^{pp} - p_{\rm DI}^{pp}\right)^2. \tag{42}$$

The probability for two-electron emission is the inclusive probability for double ionization and can be obtained with formulae similar to (39) and (40):

$$P_{\rm 2ee}^{\rm IP2} = p_{\rm DI}^{ss}\left(1 - p_{\rm SI}^{pp} - p_{\rm TI}^{pp} - p_{\rm DI}^{pp}\right)^3 + 6p_{\rm DI}^{pp}\left(1 - p_{\rm SI}^{ss} - p_{\rm TI}^{ss} - p_{\rm DI}^{ss}\right)\left(1 - p_{\rm SI}^{pp} - p_{\rm TI}^{pp} - p_{\rm DI}^{pp}\right)^2 + 3p_{\rm DI}^{sp}\left(1 - p_{\rm SI}^{sp} - p_{\rm TI}^{sp} - p_{\rm DI}^{sp}\right)\left(1 - p_{\rm SI}^{pp} - p_{\rm TI}^{pp} - p_{\rm DI}^{pp}\right)^2, \tag{43}$$

and

$$P_{\rm 2ee}^{\rm IEV} = p_{\rm DI}^{ss} + 6p_{\rm DI}^{pp}\left(1 - p_{\rm SI}^{pp} - p_{\rm TI}^{pp} - p_{\rm DI}^{pp}\right)^2 + 3p_{\rm DI}^{sp}\left(1 - p_{\rm SI}^{sp} - p_{\rm TI}^{sp} - p_{\rm DI}^{sp}\right). \tag{44}$$

In order to compare the results with the standard one-electron IPM treatment, we have also calculated the probabilities for SI and SC ($\mathtt{p}^s_{\rm SI}, \mathtt{p}^p_{\rm SI}, \mathtt{p}^s_{\rm SC}, \mathtt{p}^p_{\rm SC}$) for the single-electron processes with the active electron moving in the potential created by the proton and the Ar^+ core, described by the model potential (16). The probability for H formation is now:

$$\mathtt{P}^{\rm IPM}_{\rm H} = 2\mathtt{p}^s_{\rm SC}(1-\mathtt{p}^s_{\rm SC})(1-\mathtt{p}^p_{\rm SC})^6 + 6\mathtt{p}^p_{\rm SC}(1-\mathtt{p}^s_{\rm SC})^2(1-\mathtt{p}^p_{\rm SC})^5 \tag{45}$$

and, neglecting the simultaneous capture from different shells:

$$\mathtt{P}^{\rm IEV}_{\rm H} = 2\mathtt{p}^s_{\rm SC}(1-\mathtt{p}^s_{\rm SC}) + 6\mathtt{p}^p_{\rm SC}(1-\mathtt{p}^p_{\rm SC})^5. \tag{46}$$

Similarly, the one-electron emission probabilities are:

$$\mathtt{P}^{\rm IPM}_{\rm 1ee} = 2\mathtt{p}^s_{\rm SI}(1-\mathtt{p}^s_{\rm SI})(1-\mathtt{p}^p_{\rm SI})^6 + 6\mathtt{p}^p_{\rm SI}(1-\mathtt{p}^s_{\rm SI})^2(1-\mathtt{p}^p_{\rm SI})^5; \tag{47}$$

$$\mathtt{P}^{\rm IEV}_{\rm 1ee} = 2\mathtt{p}^s_{\rm SI}(1-\mathtt{p}^s_{\rm SI}) + 6\mathtt{p}^p_{\rm SI}(1-\mathtt{p}^p_{\rm SI})^5. \tag{48}$$

For comparison purposes, we have evaluated the probabilities for electron production (EP) (also called net ionization) in the form:

$$\mathtt{P}_{\rm EP} = 2\mathtt{p}^s_{\rm SI} + 6\mathtt{p}^p_{\rm SI}, \tag{49}$$

which includes all electron emission in the IPM approximation.[66] Assuming that only emission of one or two electrons are relevant, the results from this expression can be compared with the s-CTMC results:

$$P^{\rm IP2}_{\rm EP} = P^{\rm IP2}_{\rm 1ee} + 2P^{\rm IP2}_{\rm 2ee} \tag{50}$$

and

$$P_{\rm EP}^{\rm IEV} = P_{\rm 1ee}^{\rm IEV} + 2P_{\rm 2ee}^{\rm IEV}. \quad (51)$$

3. Results and discussion

3.1. Molecular calculations

The molecular wave functions ϕ_k and the PECs, ε_k, have been obtained in a Multi-Reference-Configuration-Interaction (MRCI) calculation with the program MELDF (see e.g. Ref. 67), modified to calculate numerically the dynamical couplings.[68] We have employed the Ar Gaussian basis set of McLean and Chandler[69] and the $(13s, 8p, 5d)$ contracted to $[5s, 4p, 2d]$ basis or Errea et al.[70] for H. Within the non-relativistic model, transitions between states with different multiplicities are not allowed and, since the entrance channel is a singlet state, we have computed the PECs and couplings in the singlet subsystem. Besides, in order to calculate the dynamical couplings, it is useful to work in the C_s subgroup. Given that the coupling operators have A' symmetry and the entrance channel also belongs to the A' irreducible representation, we have only considered $^1A'$ states, whose energies are displayed in Figure 1, and the ground-state energy is compared with the self-consistent-field (SCF) one calculated by Sidis.[71] These energies (and the corresponding wave functions) have been obtained by diagonalizing the system hamiltonian in the 3604 spin-adapted configurations generated by considering single and double excitations from the reference configurations, that correlate to Ar($3s^2 3p^6$), $Ar^+(3s^2 3p^5)$+H($1s$) and $Ar^{2+}(3s^2 3p^4)$+$H^-(1s^2)$, subject to the following rules:

- The molecular orbital correlating to Ar $3s$ orbital is always doubly occupied.
- The molecular orbitals correlating to Ar $3p$ hold between 3 and 6 electrons.
- The set of molecular orbitals correlating to H(n =1, 2 and 3) can hold up to 2 electrons.
- The molecular orbitals correlating to Ar $4s$ and $4p$ orbitals can hold up to 1 electron.

These rules aim at producing a relatively small number of configurations that have the lowest possible energies while they do not allow more than two electrons in the set of molecular orbitals that correlate to Hydrogen atomic orbitals. The molecular orbitals have been obtained in a previous restricted-Hartree-Fock calculation.

The most conspicuous fact of this diagram is that the energies of the DC channels H^-+Ar^{2+} lie above the ionization threshold $H^++Ar^+(^2P^o)$;[59] i.e., the molecular states above this limit correspond to a discretization of the molecular ionization continuum in the L^2-integrable basis.

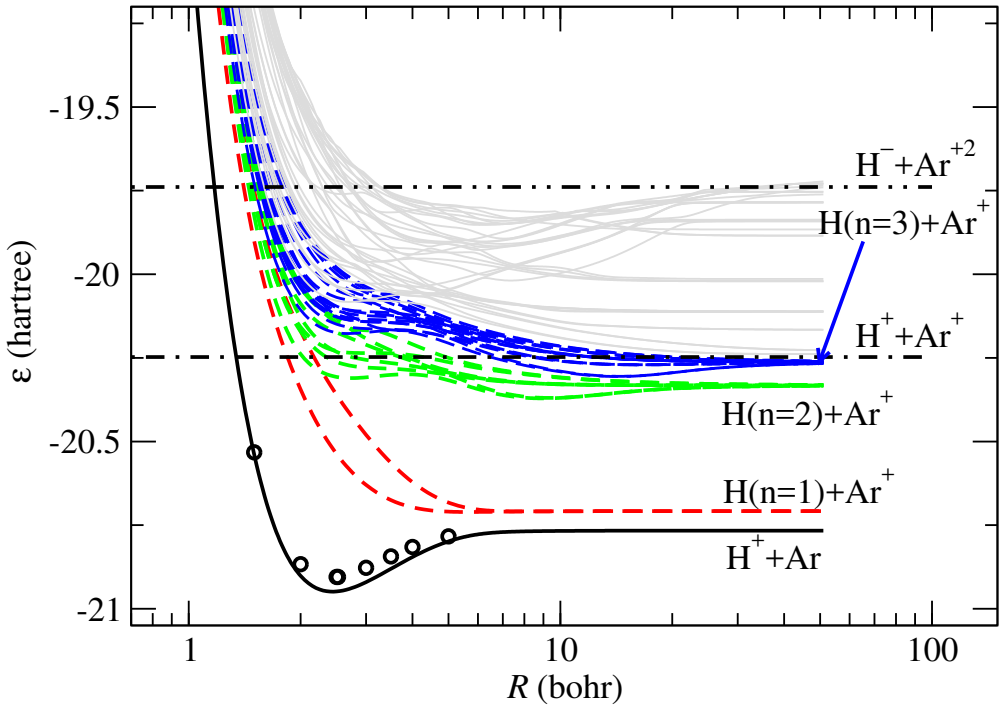

Figure 1: Potential energy curves of the $^1A'$ electronic states of the ArH^+ quasimolecule. The thick full-line is the energy of the collision entrance channel, while the circles are the data calculated by Sidis;[71] the dashed lines are the energies of the states dissociating into $H+Ar^+$. The thin solid lines are other states correlating to excitation, single or double electron capture. The energies of the $H^++Ar^+(^2P^o)$ ionization threshold and the channel $H^-+Ar^{2+}(^1S)$ are also indicated in the figure.

From inspection of the PECs, one expects that the probabilities for populating the SC states, which are the first excited states, will be relatively high in comparison to that of populating the DC states, which are very excited and are found above a series of excitation

and SC states. The first step in the SC mechanism is the transition, at $R \simeq 6$ bohr, from the ground state to the first and second excited states that dissociate into $H(n=1)+Ar^+(^2P^o)$. Part of the population of these two states is then transferred to other molecular states at shorter distances, leading to SC into hydrogen excited states.

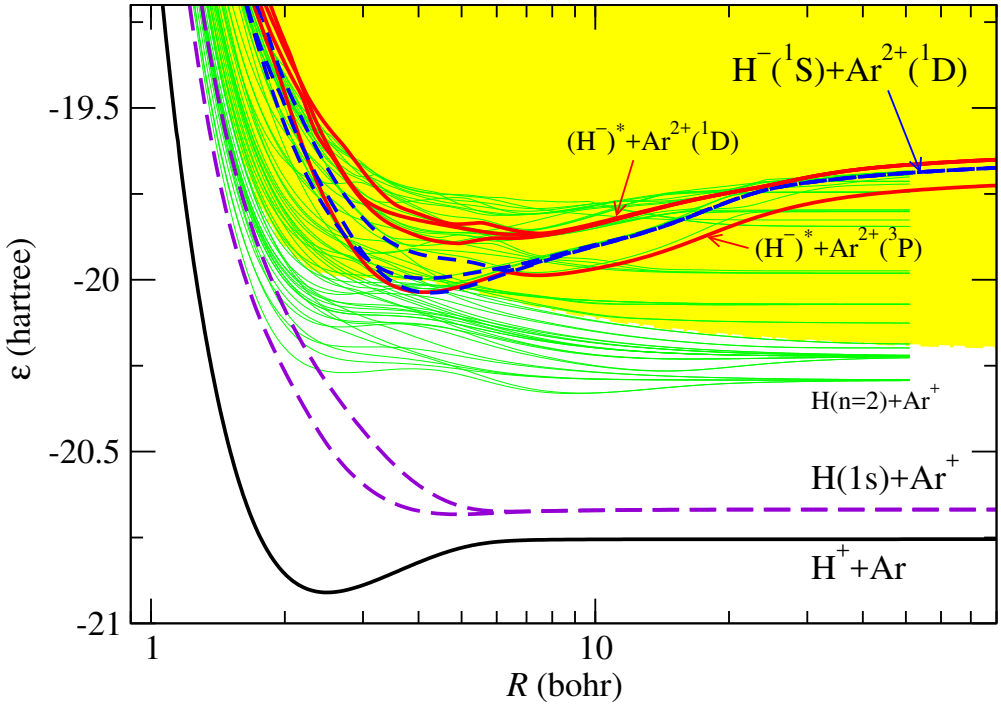

Figure 2: Potential energy curves of the $^1A'$ electronic states of the ArH^+ quasimolecule, calculated using the block-diagonalization method (thick solid– and dashed–lines). The thin solid-lines are those of Figure 1. The shaded area indicates the energies above the ArH^+ ionization threshold.

Assuming that the collision characteristic time is large compared to the autoionization lifetime, it is possible to calculate the DC cross section with the molecular basis of Figure 1. However, it requires to identify the molecular states dissociating into $H^-(^1S)+Ar^{2+}(^1D)$, whose energies show many avoided crossings with that of the continuum and Rydberg states. To overcome this difficulty, we have considered an alternative basis of states by using a BD technique similar to that employed in collisions of multicharged ions with H_2.[72–74] In this technique, we diagonalize the Hamiltonian matrix in the subspace that does not include the molecular Rydberg series dissociating into $H^*+Ar^+(^2P^o)$. In practice, our CI basis excludes

configurations where the molecular orbitals that correlate to H($n \geq 3$) are singly occupied. As before, we consider a set of reference configurations that describe the entrance channel, the SC channel to H($n = 1, 2$), and the DC channel, and generate a list of additional configurations subject to the rules:

- The molecular orbital correlating to Ar $3s$ orbital has a minimum of 1 electron.
- The molecular orbitals correlating to Ar $3p$ hold between 3 and 6 electrons.
- The set of molecular orbitals correlating to H orbitals with n =1, 2 and 3 always hold 2 electrons, in order to exclude the Rydberg molecular states.
- The molecular orbital correlating to Ar $4s$ and $4p$ orbitals can hold up to 1 electron.

The final CI space has 4366 spin-adapted configurations. We have obtained the lowest 30 adiabatic roots of the corresponding hamiltonian. These states have been diabatized following Errea et al.[74] to remove only very narrow avoided crossings and 10 states, out of the initial 30, have been selected to carry out the eikonal calculation. The 10 selected states are plotted with solid and dashed thick lines in Figure 2. In that figure, the thin lines correspond to the energies of the excited states calculated without using the BD restriction. It must be noted that our calculation yields three molecular states (thick-dashed lines in Figure 2) that correlate to the bound state of H^- and several excited channels, (thick-full lines) that correlate to states of H^- above the ionization threshold; they are discretized representations of H^- continuum, but we have kept them in the scattering CI basis set because their PECs exhibit avoided crossings with those of the asymptotically bound states.

3.2. MFCC calculations

At low collision energies, the target ionization is unimportant and the experimental cross sections of H formation can be compared to the calculations of SC. As the impact energy increases, SI and TI become relevant and the MFCC method cannot be applied. We compare

in Figure 3 our total SC cross sections calculated with the 10 molecular wave functions described above. This basis includes only two states to account for the electron capture to H($n = 1$), but we have checked that including the channels that dissociate into Ar^++H($n = 2$) and Ar^++H($n = 3$) does not change the total SC cross section in more than 2%. This feature is also found in calculations performed with molecular wave functions including SC channels up to H($n = 3$), obtained without the BD procedure. We find good agreement between the MFCC cross section and the experiments for $E \lesssim 8$ keV. At these energies, our calculations clearly show better agreement with the experiment than that of Kirchner et al.[35] and Fremont,[23] but it overestimates some experimental values for $8 < E < 10$ keV, where ionization starts to be sizable (see Figure 7). Only the END calculation of Cabrera-Trujillo et al.[38] has provided total SC cross sections for $E < 1$ keV, but their values lie below the experiments and our curve for $E > 200$ eV.

In Figure 4 we plot the total cross section for H^- formation. At low energies, the H^- is formed in the DC process (3), and it is expected that the contribution of three-electron processes as (5) is very small, as was pointed out in the pioneering work of Williams.[11] The semiclassical calculation has been carried out with the 10-states basis set that includes the ground state, the two states leading to SC into Ar^++H($n = 1$), and seven states that asymptotically dissociate into Ar^{2+}+H^-; three of them dissociate into the lowest (bound) electronic state of H^- (see Figure 2), while the others lead to excited H^-, which will eventually autoionize.

The inspection of the time evolution of the populations $|a_k|^2$ from (9) poins out that the DC states are populated through a two-step mechanism via a first transition to the SC states. In fact, the total cross section calculated without SC states is an order of magnitude smaller than the one shown in Figure 4. As the energy increases, the transitions to other SC and excitation channels become relevant and the BD basis is not appropriate. In the illustration of Figure 4 we have limited the energy range to $E \leq 5$ keV, since at $E = 5$ keV our cross section is clearly higher than the experimental values.[10,11,13,17] The first maximum of the

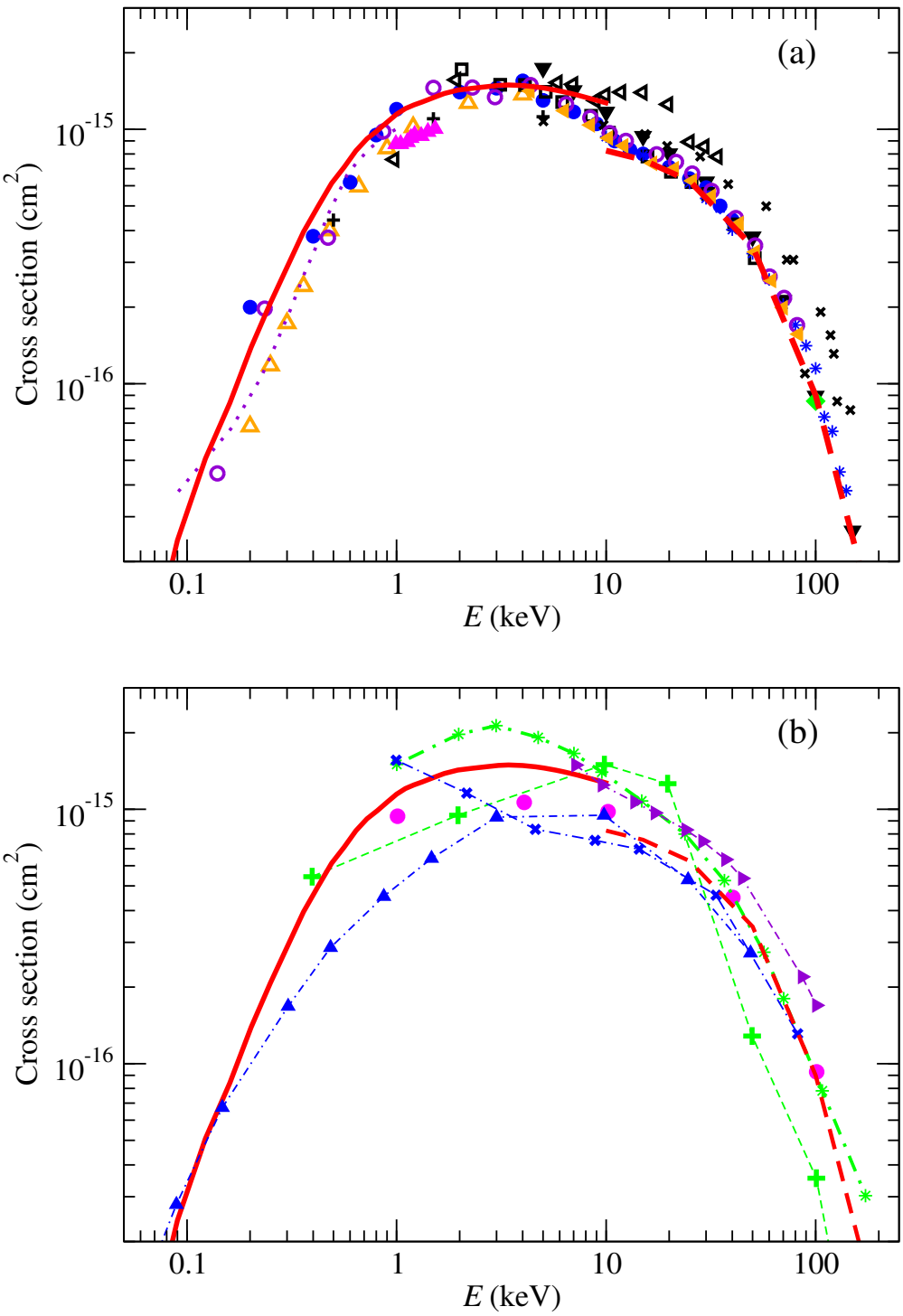

Figure 3: Total cross section as function of the collision energy for H formation in H^++Ar collisions. (a) Present calculations: Full line, MFCC calculation; dashed line, s-CTMC calculation [Eq. (34)], compared to experimental results: ○;[75] ◀;[24] ●;[25] ×;[10] ◁;[76] □;[26] (···);[27] +;[77] ∗;[78] ♦;[28] ▲;[30] ▼;[31] △.[32] (b) Present results compared to previous calculations: (−·−∗−·), BGM-IPM;[36] (−·− ▶ −·), AOCC-IPM;[37] (−·−▲−·), END;[38] (−·− × −·), AOCC-IPM;[38] ●, TDDFT;[21] (- - + - -), CTMC.[23]

experimental cross sections at $E \approx 5$ keV is not reproduced by our MFCC calculation since the above-mentioned transitions to states not included in the basis produce an overpopulation of the DC channels. For $E \leq 3$ keV, we obtain good agreement with the experiments of Morgan and Eriksen[13] and Martinez et al.,[17] and our results are higher than that of Williams.[11]

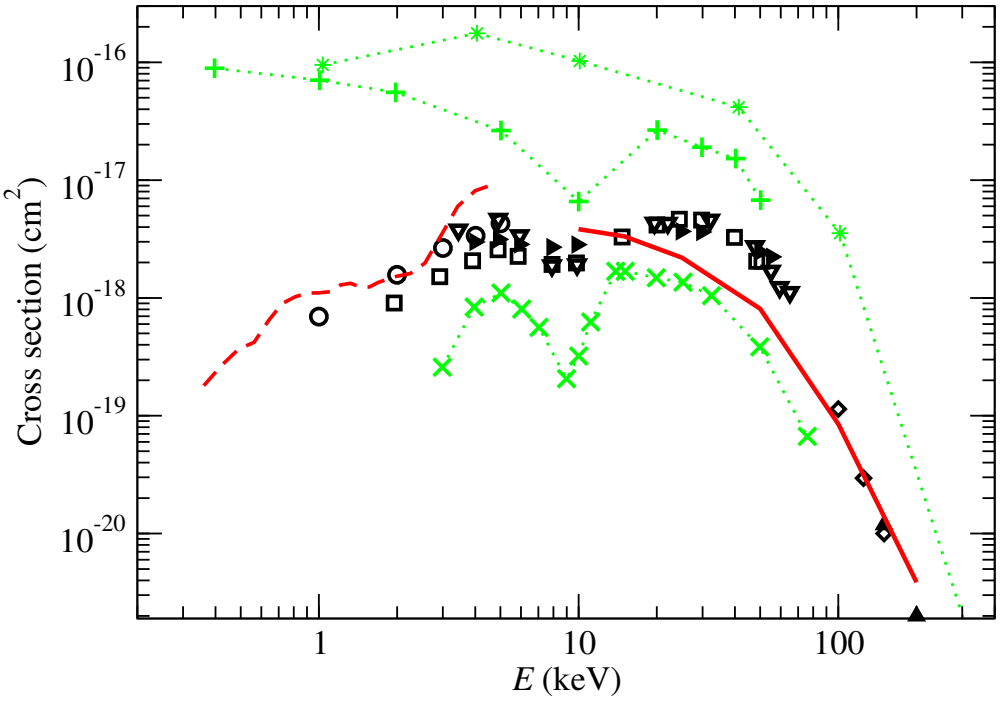

Figure 4: Total cross section as function of the collision energy for H^- formation in H^++Ar collisions. Present results: dashed line, MFCC calculation; full line, s-CTMC calculation [Eq. (40)]. Experimental results: ▶;[10] □;[11] ◇;[12] ▽;[13] ▲;[14] ○.[17] Previous calculations: (· · · × · · ·);[17] (· · · ∗ · · ·);[21] (· · · + · · ·).[23]

A stringent test of the MFCC calculation is provided by the comparison of the calculated differential cross sections for DC with the measured values of Martinez et al.[17] (see Figure 5). In the calculation we have applied the stationary phase expression (14) with the transition probabilities for population of the DC channels obtained with the BD basis set. Considering that the total cross section deviates from the experiment at $E \geq 5$ keV, we present the calculations at $E = 1$ and $E = 3$ keV. Since the PEC of the ground molecular state has a minimum, the classical deflection function exhibits a rainbow at $\theta_r \leq 0.37°$ for these

energies. Given that the expression (14) does not take into account the interference between the trajectories leading to the same scattering angle, the calculation is limited to $\theta > \theta_r$. We have checked that our elastic deflection function at $E = 1$ keV is practically identical to that of Sidis,[71] in accordance with the good comparison of the corresponding ground-state potentials plotted in Figure 1. On the other hand, the calculation of transition probabilities for large scattering angles (small impact parameters) involves PECs and couplings at small internuclear distances. At these short distances, the presence of many avoided crossings precludes the identification of the molecular states and the truncation of the basis. Besides, the BD technique is based on the asymptotic character of the molecular orbitals, which has no meaning at short internuclear distances. Our calculation has considered impact parameters larger than $b = 0.7$ bohr, leading to the differential cross sections for $\theta < 2^\circ$ of Figure 5. In this respect, it must be noted that the calculation of differential cross sections at $E > 5$ keV would involve smaller distances.

From inspection of Figure 5, one can note that, in spite of the simple method employed, the estimate of the differential cross sections at $E = 1$ keV correctly reproduces the order of magnitude and the angle dependence of the measurements, while the statistical model of Juhász[40] systematically overestimates the experimental cross section. The shape of the cross section is determined by that of the classical elastic cross section, with some structures, due to the oscillations of the transition probabilities. These structures might be smeared out by increasing the basis size, and are difficult to observe in the experiment that has a resolution of 0.1 degree. At $E = 3$ keV the calculation overestimates the experimental cross section for $\theta > 0.5^\circ$ probably because of the lack of molecular states which are populated at low internuclear distances, removing part of the population of the DC states. Although this difficulty is not relevant in the calculation of the total cross section, it indicates the main limitation of our model, in particular in order to extent the calculation to high impact energies.

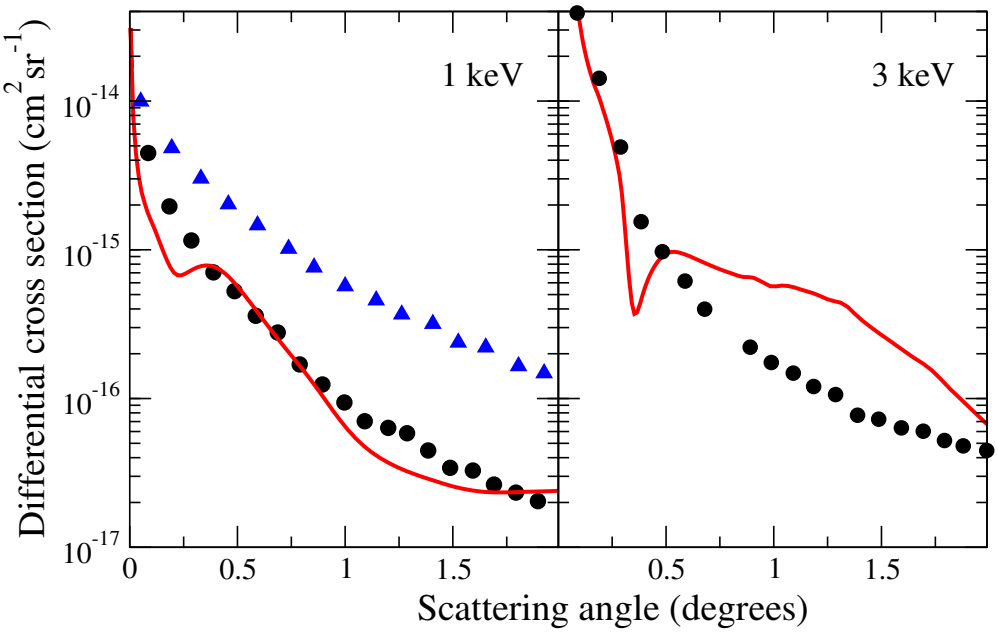

Figure 5: Differential cross section for double electron capture as function of the scattering angle in H^++Ar collisions for $E = 1$ and 3 keV. Full lines, present results. ▲, results of Juhász[40] for $E = 1$ keV. •, experimental results of Martinez et al.[17]

3.3. CTMC calculations for H and H^- formation

The total cross sections for H production, calculated with the s-CTMC and the IEVM interpretation (34) are plotted in Figure 3. The present calculations agree with the experimental results of Refs. 75, 24, 78, 28 and 31 for $E \gtrsim 25$ keV, which supports our method at these energies. Our results also agree with the calculations of Refs. 36 and 21 for $25 \lesssim E \lesssim 100$ keV. Although our MFCC and s-CTMC calculations cover a wide energy range, the two calculations do not merge because of the limitations of the MFCC at energies where ionization is relevant, as well as the difficulties of the classical methods at low energies. In one-electron systems, the CCAO methods are appropriate to cover the energies near the maximum of the SC total cross section (see Ref. 79). For H^+ + Ar collisions, the main limitation of the CCAO methods is the use of the IPM approximation. However, the good agreement of the results of Amaya-Tapia et al. (CCAO-IPM)[37] and Kirchner et al.[36] (BGM-IPM) with the 8-electron MFCC calculation and with the experiment of Rudd et al.[31] at $E = 10$ keV,

indicates that these CCAO calculations are reliable at $E \simeq 10$ keV (see also the low-energy range of Figure 6). At $E = 10$keV, the TDDFT cross section of Wang et al.[21] is below the the CCAO results[36,37] and it is close to the s-CTMC value.

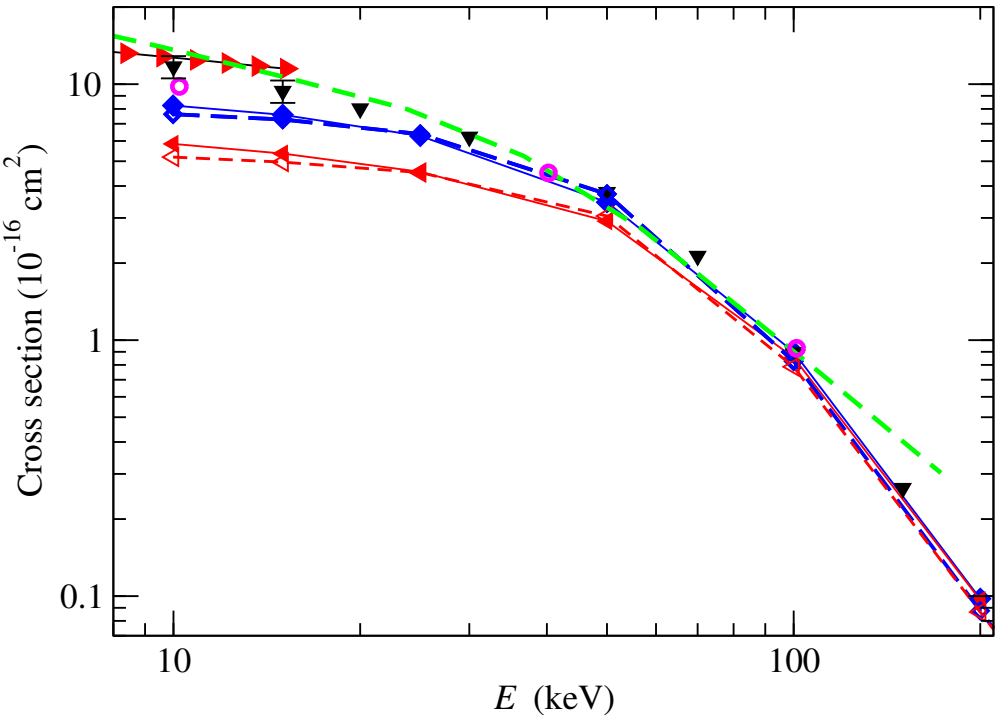

Figure 6: Total cross section for H formation as function of the collision energy in H^++Ar collisions. Present calculations: (—♦—), s-CTMC with IEVM interpretation [Eq. (34)]; (—◀—), s-CTMC with IP2 interpretation [Eq. (33)]; (– – ◊ – –), one-electron CTMC with IEVM interpretation [Eq. (46)]; (- -◁ - -), one-electron CTMC with IPM interpretation [Eq. (45)]; (—▶—), MFCC calculation. The experimental results of Rudd et al.[31](▼) are included for comparison. Other experimental data are shown in Figure 3. Previous calculations of Refs. 36 (– – –) and 21 are also included.

In order to further explore the workings of the s-CTMC calculations, we compare in Figure 6 the cross sections for H production obtained with the s-CTMC and with the standard one-electron-CTMC calculation, both with the same model potentials. In the s-CTMC we consider the two interpretations given by Eqs. (33) and (34), and the corresponding expressions (45) and (46), in terms of the one-electron probabilities for single capture and ionization. The results displayed in Figure 6 show that s-CTMC and one-electron-CTMC calculations agree for $10 < E < 200$ keV when using the same many-electron interpretation,

which support both calculations. For $E < 50$ keV, we find differences between the two interpretations, and the IEVM shows better agreement with the experiments than the IPM one.

The s-CTMC total cross section for H^- formation is plotted in Figure 4. As in Figure 3, we only plot the IEVM result of Eq. (40). Our cross sections agree with the high-energy experiments[12,14] for $E \geq 100$ keV. Since previous calculations of the cross section for H^- formation are unsatisfactory, our s-CTMC represents a significant improvement. However, our calculation is not able to reproduce the two maxima structure of the experimental cross sections. The first maximum at $E \simeq 5$ keV is not reproduced because of the difficulties of the MFCC calculation explained in subsection 3.2 . With respect to the second maximum, at $E \approx 30$ keV, we find that the s-CTMC results underestimate the experimental ones[10–13] by a about a factor of two. The pioneering work of Williams[11] explained the maximum at $E \approx 25$ keV as due to the three-electron process (5). One can note that our formulae (39), (40) include the probability for this process; for instance, the second term of (40) is:

$$6p_{\rm DC}^{pp}\left(1-p_{\rm SC}^{pp}-p_{\rm TI}^{pp}-p_{\rm DC}^{pp}\right)^2 = 6p_{\rm DC}^{pp}\left(p_{\rm E}^{pp}+p_{\rm SI}^{pp}+p_{\rm DI}^{pp}-p_{\rm DC}^{pp}\right)^2 \tag{52}$$

The leading term is $6p_{\rm DC}^{pp}p_{\rm E}^{pp}$, but it contains the product $p_{\rm DC}^{pp}p_{\rm E}^{pp}p_{\rm SI}^{pp}$ that correspond to the reaction where two electrons are exchanged and a third electron is emitted. This description is probably not accurate, taking into account that our method explicitly considers two-electron processes, and the probabilities for three-electron reactions are obtained by multiplying the probabilities from the two-electron calculation. This limitation is similar to that found in the one-electron CTMC in calculating the probabilities for two-electron processes by multiplying one-electron probabilities.

3.4. CTMC calculations for electron production

The EP is the dominant process for $E > 25$ keV, and the large probabilities allow us to extend the CTMC calculations up to $E = 400$ keV with the same statistics employed for $E \leq 200$ keV. In general, the CTMC calculations with initial microcanonical distributions yield accurate ionization cross sections with the exception of the ionization threshold, where the transitions from the classically forbidden region of the quantal distribution are particularly relevant, although this problem is much less important for processes starting from excited shells.[80,81] In order to discuss the accuracy of the microcanonical calculations, we compare in Figure 7 the results from Eq. (49) with previous calculations and experiments. Note that a linear scale has been used in Figure 7 to ease the comparisons. The one-electron CTMC cross section is lower than the experimental one for $E = 30$ keV, probably because of the use of the microcanonical distribution, but the effect is not large, and the total cross section agrees with the one-electron calculation of Ref. 35. For $E > 30$ keV, the standard one-electron CTMC calculation [Eq. (49)] overestimates the experimental values although the discrepancy near the maximum is relatively small compared to the uncertainties ($\pm$ 10^{-16} cm^2) of the experimental values, indicating that the difficulties in representing DI and TI processes are not very important in this calculation. The cross section from the CTMC calculation agrees with that of Kirchner et al.[35] using the so-called response approximation. Kirchner et al.[35] discussed that their calculation, and also the present one, does not include the autoionization contribution to the EP. They estimated this contribution by considering the probabilities of excitation to doubly-excited states in the IPM, which leads to large cross sections that are probably overestimated.

The results of applying the s-CTMC with the IP2 interpretation (50) agree with the experiment for $E > 20$ keV, which indicates that the contribution from two-electron processes is improved in the s-CTMC treatment. However, the use of the IEVM interpretation (51) leads to a large total cross section that suggests that the complete neglect of simultaneous electron removal from different subshells is too restrictive for the EP process.

In order to understand the different behavior of the IEVM (34), (42), and IP2 (33), (41) formulae of H and electron production we start by considering the first term of (33):

$$\left(p_{\rm SC}^{ss}+p_{\rm TI}^{ss}\right)\left(1-p_{\rm SC}^{pp}-p_{\rm TI}^{pp}-p_{\rm DC}^{pp}\right)^3 .$$

The IP2 approximation is based on the assumption that the removal of the second electron (a p electron in this example) is not influenced by that of the first one (the s electron). The calculations at $E \lesssim 30$ yield $p_{\rm SC}^{ss} \approx p_{\rm SC}^{pp}$ and these probabilities reach values larger than 0.25, with small probabilities for the other capture and ionization processes. Accordingly, at the lowest energies of Figure 6, the factor $\left(1-p_{\rm SC}^{pp}-p_{\rm TI}^{pp}-p_{\rm DC}^{pp}\right)^3$ leads to an important reduction of $P_{\rm H}^{\rm IP2}$. The alternative IEVM formula (34) assumes that the probability of removing the second electron from a different subshell is not physical, since it corresponds to extract an electron from a singly-charged cation. The equation (34) takes $p_{\rm SC}^{pp}=0$ in (53), which corresponds to a limit situation applicable when the capture probabilities are large, as found in Figure 6. Similarly, in the standard one-electron treatment, the IEVM approach (46) is more appropriate than the IPM one (45).

On the other hand, the first term of the IP2 probability for one-electron production (41) is

$$\left(p_{\rm SI}^{ss}+p_{\rm TI}^{ss}\right)\left(1-p_{\rm SI}^{pp}-p_{\rm TI}^{pp}-p_{\rm DI}^{pp}\right)^3 .$$

In this case, the calculations lead to $p_{\rm SI}^{ss} \approx p_{\rm SI}^{pp}/2$ for $E \leq 100$ keV. The relatively small ionization probability from the $3s$ subshell ($\lesssim 0.15$) will be of little significance to avoid ionization from the $3p$ subshell, which explains that the IEVM is too stringent to calculate the one-electron production probability.

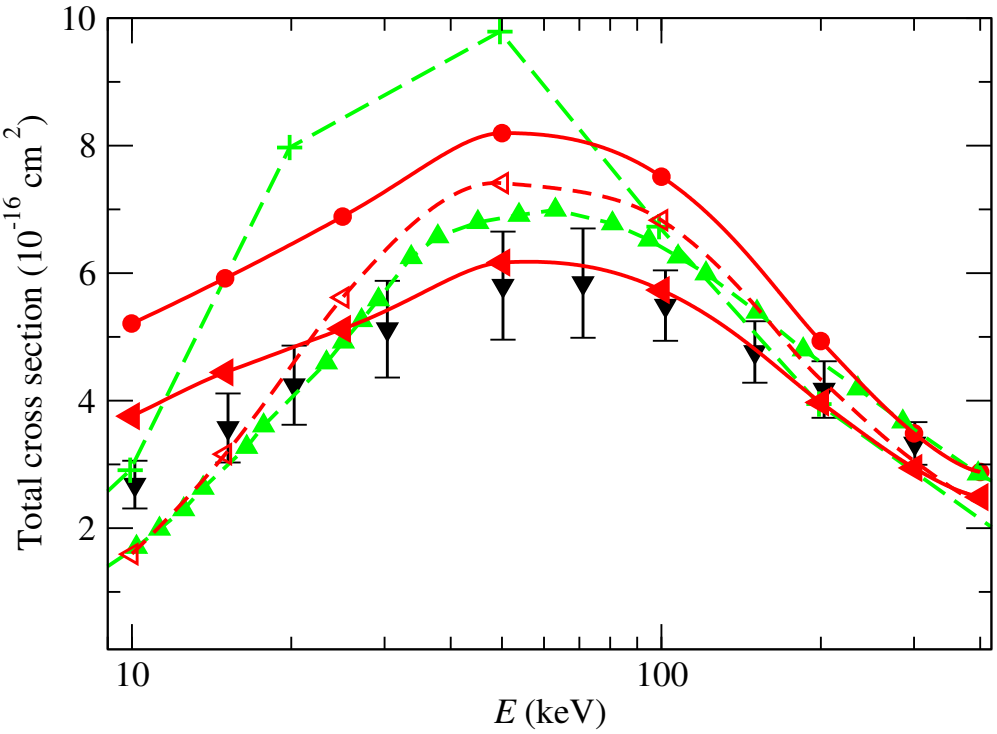

Figure 7: Total cross section for electron production as function of the collision energy in H^++Ar collisions. Present calculations: (—●—), s-CTMC with IEVM interpretation [Eq. (51)]; (—◀—); s-CTMC with IP2 interpretation [Eq. (50)]; (– ◁ –), one-electron CTMC [Eq. (49)]. Recommended data: ▼.[82] Previous calculations: (– ▲ –);[35] (– + –).[23]

4. Summary

We have reported calculations of cross sections for capture and ionization processes in proton+Ar collisions. This collision system has been studied in several experimental works, but the calculations are not able to accurately represent two-electron processes. We have applied two methods. At low energy (100 eV$< E <$ 10 keV), the ionization is not competitive with the electron capture process, and we have employed an expansion in a molecular basis set, which leads to cross sections for H formation in good agreement with the experiments for these energies. Indeed, the difference between the cross section for H-formation and the experimental data at $E \approx 20$ keV is close to the experimental EP cross section, which points out that the MFCC yields the cross section for Ar electron-loss. The two-electron capture has been described by applying a block-diagonalization method to calculate the molecular autoionizing functions that dissociate into H^-+ $Ar^{2+}(^1D)$. Although the total cross sections are very small (of the order of 10^{-18} cm^2), our semiclassical values present reasonably good agreement with the experimental ones. The differential cross sections for double electron capture have been estimated using a stationary-phase approximation. The calculation shows that the shape of the experimental cross section as function of the scattering angle is given by the classical dispersion in the potential of the ground electronic state of the ArH^+ molecule. The non-adiabatic transitions introduce some narrow structures. The main limitation of this calculation is the difficulty of describing the transitions at large scattering angles.

The calculation at intermediate energies has been carried out by applying the s-CTMC method, which has been successfully implemented for two-electron systems in Ref. 41. We have checked that the s-CTMC yields cross sections for H formation very close to that obtained in the standard, one-electron CTMC treatment with the same model potential, but the method improves the results for H^- formation, which in the standard one-electron CTMC are overestimated by almost one order of magnitude. The main limitation of the technique is the uncertainty in the calculation of many-electron probabilities involving several (sub)shells. This difficulty is relevant at relatively low collision energies, and also limits the application

of the conventional one-electron CTMC method. Our results for H^++Ar collisions show that the IEVM formulae are preferable for H^-- and H-formation reactions for $10 \lesssim E \lesssim 50$ keV, while IP2 and IEVM interpretations agree for $E \gtrsim 50$ keV. The electron-production process is in general better described by the IP2 interpretation.

Acknowledgement

This work has been partially supported by Ministerio de Economía and Competitividad (Spain), project no. ENE2014-52432-R. We thank Prof. J-Y. Chesnel and B. Sulik, and Dr. Z. Juhász for helpful discussions. The Centro de Computación Científica of UAM is akcnowledged for the computational hosting facilities.

References

(1) Larsson, M.; Geppert, W. D.; Nyman, G. Ion Chemistry in Space. *Reports on Progress in Physics* **2012**, *75*, 066901.

(2) Millar, T. J.; Walsh, C.; Field, T. A. Negative Ions in Space. *Chemical Reviews* **2017**, *117*, 1765–1795, PMID: 28112897.

(3) Glover, S. C.; Savin, D. W.; Jappsen, A.-K. Cosmological Implications of the Uncertainty in H^- Destruction Rate Coefficients. *The Astrophysical Journal* **2006**, *640*, 553.

(4) Bourgalais, J.; Jamal-Eddine, N.; Joalland, B.; Capron, M.; Balaganesh, M.; Guillemin, J.-C.; Picard, S. D. L.; Faure, A.; Carles, S.; Biennier, L. Elusive anion growth in Titans atmosphere: Low temperature kinetics of the C_3N^-+HC_3N reaction. *Icarus* **2016**, *271*, 194 – 201.

(5) Shuman, N. S.; Miller, T. M.; Bemish, R. J.; Viggiano, A. A. Electron-Catalyzed Mutual

Neutralization of Various Anions with Ar^+: Evidence of a New Plasma Process. *Phys. Rev. Lett.* **2011**, *106*, 018302.

(6) Kakati, B.; Kausik, S. S.; Bandyopadhyay, M.; Saikia, B. K.; Kaw, P. K. Development of a novel surface assisted volume negative hydrogen ion source. *Scientific Reports* **2017**, *7*, 11078.

(7) Almeida, D.; Antunes, R.; Martins, G.; García, G.; McCullough, R.; Eden, S.; Limão-Vieira, P. Mass spectrometry of anions and cations produced in 1–4 keV H, O, and OH collisions with nitromethane, water, ethanol, and methanol. *International Journal of Mass Spectrometry* **2012**, *311*, 7 – 16.

(8) Oller, J. C.; Ellis-Gibbings, L.; da Silva, F. F.; Limão-Vieira, P.; García, G. Novel experimental setup for time-of-flight mass spectrometry ion detection in collisions of anionic species with neutral gas-phase molecular targets. *EPJ Techniques and Instrumentation* **2015**, *2*, 13.

(9) Fogel', Y. M. The production of negative ions in atomic collisions. *Soviet Physics Uspekhi* **1960**, *3*, 390.

(10) Afrosimov, V.; Ilin, R.; Solovev, E. Electron Capture by Protons in Inert Gases. *Sov. Phys. Tech. Phys.* **1960**, *5*, 661–666.

(11) Williams, J. F. Cross Sections for Double Electron Capture by 2-50-keV Protons Incident upon Hydrogen and the Inert Gases. *Phys. Rev.* **1966**, *150*, 7–10.

(12) Toburen, L. H.; Nakai, M. Y. Double-Electron-Capture Cross Sections for Incident Protons in the Energy Range 75 to 250 keV. *Phys. Rev.* **1969**, *177*, 191–196.

(13) Morgan, T. J.; Eriksen, F. J. Single- and double-electron capture by 1-100-keV protons in collisions with magnesium and barium atoms. *Phys. Rev. A* **1979**, *19*, 1448–1456.

(14) Almeida, D. P.; de Castro Faria, N. V.; Freire, F. L.; Montenegro, E. C.; de Pinho, A. G. Collisional formation and destruction of fast negative hydrogen ions in He, Ne, and Ar targets. *Phys. Rev. A* **1987**, *36*, 16–25.

(15) Li, B.; Ma, X.; Zhu, X. L.; Zhang, S. F.; Liu, H. P.; Feng, W. T.; Qian, D. B.; Zhang, D. C.; Chen, L.; Brédy, R. et al. High negative ion production yield in 30 keV F^{2+}+adenine ($C_5H_5N_5$) collisions. *Journal of Physics B: Atomic, Molecular and Optical Physics* **2009**, *42*, 075204.

(16) Tybislawski, M.; Bends, M.; Berger, R. J.; Hettlich, M.; Lork, R.; Neuwirth, W. Production of negatively charged fragments in collisions of swift positive hydrogen ions with molecules. *Zeitschrift für Physik D Atoms, Molecules and Clusters* **1993**, *28*, 49–59.

(17) Martinez, H.; Alarcon, F. B.; Amaya-Tapia, A. Double capture cross sections in p-Ar collisions. *Phys. Rev. A* **2008**, *78*, 062715.

(18) Angelin, E. J.; Hippler, R. Superoxide-anion formation in collisions of positively charged argon ions with oxygen molecules. *Phys. Rev. A* **2013**, *87*, 052704.

(19) Juhász, Z.; Sulik, B.; Rangama, J.; Bene, E.; Sorgunlu-Frankland, B.; Frémont, F.; Chesnel, J.-Y. Formation of negative hydrogen ions in 7-keV OH^++Ar and OH^++acetone collisions: A general process for H-bearing molecular species. *Phys. Rev. A* **2013**, *87*, 032718.

(20) Lattouf, E.; Juhász, Z.; Chesnel, J.-Y.; Kovács, S. T. S.; Bene, E.; Herczku, P.; Huber, B. A.; Méry, A.; Poully, J.-C.; Rangama, J. et al.Formation of anions and cations via a binary-encounter process in OH^++Ar collisions: The role of dissociative excitation and statistical aspects. *Phys. Rev. A* **2014**, *89*, 062721.

(21) Wang, F.; Xu, X.; Hong, X.; Wang, J.; Gou, B. A theoretical model for electron transfer in ion–atom collisions: Calculations for the collision of a proton with an argon atom. *Physics Letters A* **2011**, *375*, 3290 – 3295.

(22) Chesnel, J.-Y.; Juhász, Z.; Lattouf, E.; Tanis, J. A.; Huber, B. A.; Bene, E.; Kovács, S. T. S.; Herczku, P.; Méry, A.; Poully, J.-C. et al. Anion emission from water molecules colliding with positive ions: Identification of binary and many-body processes. *Phys. Rev. A* **2015**, *91*, 060701.

(23) Frémont, F. Electron capture and single ionization in H^++Ar collisions: classical calculations. *Journal of Physics B: Atomic, Molecular and Optical Physics* **2016**, *49*, 065206.

(24) Stier, P. M.; Barnett, C. F. Charge Exchange Cross Sections of Hydrogen Ions in Gases. *Phys. Rev.* **1956**, *103*, 896–907.

(25) Allison, S. K. Experimental Results on Charge-Changing Collisions of Hydrogen and Helium Atoms and Ions at Kinetic Energies above 0.2 kev. *Rev. Mod. Phys.* **1958**, *30*, 1137–1168.

(26) Williams, J. F.; Dunbar, D. N. F. Charge Exchange and Dissociation Cross Sections for H_1^+, H_2^+, and H_3^+ Ions of 2- to 50-keV Energy Incident Upon Hydrogen and the Inert Gases. *Phys. Rev.* **1966**, *149*, 62–69.

(27) Koopman, D. W. Measurement of Charge-Exchange Cross Sections for H^+, H_2^+, and He^+ Ions. *Phys. Rev.* **1967**, *154*, 79–85.

(28) Toburen, L. H.; Nakai, M. Y.; Langley, R. A. The measurement of high-energy charge transfer cross sections for incident protons and atomic hydrogen in various gases and the K-, L-, and M-Auger, L-Coster-Kronig and the conversion electron spectra of platinum in the decay of 195Au. Ph.D. thesis, 1967.

(29) Abignoli, M.; Barat, M.; Baudon, J.; Fayeton, J.; Houver, J. C. Differential measurements on ion-atom collisions in the energy range 500–3000 eV. IV. H+noble gas atom collisions. *Journal of Physics B: Atomic and Molecular Physics* **1972**, *5*, 1533.

(30) Latypov, Z. Z.; Shaporenko, A. A. Proton recharge on atoms of innert gases at 80-1500 eV collision energies. *Zh. Tekh. Fiz.* **1976**, *46*, 2178–2181 [Sov. Phys. Tech. Phys. **21**, 1277 (1976)].

(31) Rudd, M. E.; DuBois, R. D.; Toburen, L. H.; Ratcliffe, C. A.; Goffe, T. V. Cross sections for ionization of gases by 5-4000-keV protons and for electron capture by 5-150-keV protons. *Phys. Rev. A* **1983**, *28*, 3244–3257.

(32) Kusakabe, T.; Sakaue, H. A.; Tawara, H. Charge-Transfer Cross Sections of H^+ Ions in Collisions with Noble Gas Atoms in the Energy Range below 4.0 keV. *Plasma and Fusion Research* **2011**, *6*, 2401102–2401102.

(33) DuBois, R. D.; Toburen, L. H.; Rudd, M. E. Multiple ionization of rare gases by H^+ and He^+ impact. *Phys. Rev. A* **1984**, *29*, 70–76.

(34) Kirchner, T.; Gulyás, L.; Lüdde, H. J.; Henne, A.; Engel, E.; Dreizler, R. M. Electronic Exchange Effects in $p+\mathrm{Ne}$ and $p+\mathrm{Ar}$ Collisions. *Phys. Rev. Lett.* **1997**, *79*, 1658–1661.

(35) Kirchner, T.; Horbatsch, M.; Lüdde, H. J. Time-dependent independent-particle model calculation of multiple capture and ionization processes in $p-\mathrm{Ar}$, $\overline{p}-\mathrm{Ar}$, and $\mathrm{He}^{2+}-\mathrm{Ar}$ collisions. *Phys. Rev. A* **2002**, *66*, 052719.

(36) Kirchner, T.; Horbatsch, M.; Keim, M.; Lüdde, H. J. State-selective electron-capture calculations for p-Ar collisions in an independent many-electron model. *Phys. Rev. A* **2004**, *69*, 012708.

(37) Amaya-Tapia, A.; Martínez, H.; Hernández-Lamoneda, R.; Lin, C. D. Charge transfer in $H^+ + \mathrm{Ar}$ collisions from 10 to 150 keV. *Phys. Rev. A* **2000**, *62*, 052718.

(38) Cabrera-Trujillo, R.; Amaya-Tapia, A.; Antillón, A. Differential, state-to-state, and total-charge-transfer cross sections for H^+ colliding with Ar. *Phys. Rev. A* **2009**, *79*, 012712.

(39) Abrines, R.; Percival, I. C. Classical theory of charge transfer and ionization of hydrogen atoms by protons. *Proceedings of the Physical Society* **1966**, *88*, 861.

(40) Juhász, Z. Thermodynamic model for electron emission and negative- and positive-ion formation in keV molecular collisions. *Phys. Rev. A* **2016**, *94*, 022707.

(41) Jorge, A.; Illescas, C.; Méndez, L.; Pons, B. Switching classical trajectory Monte Carlo method to describe two-active-electron collisions. *Phys. Rev. A* **2016**, *94*, 022710.

(42) Spranger, T.; Kirchner, T. Auger-like processes in multiple ionization of noble gas atoms by protons. *Journal of Physics B: Atomic, Molecular and Optical Physics* **2004**, *37*, 4159.

(43) Galassi, M. E.; Rivarola, R. D.; Fainstein, P. D. Multiple electron emission from noble gases colliding with proton beams, including postcollisional effects. *Phys. Rev. A* **2007**, *75*, 052708.

(44) Mó, O.; Riera, A.; Yáñez, M. Calculation of radial couplings in the model-potential and pseudopotential approaches: The NaH quasimolecule. *Phys. Rev. A* **1985**, *31*, 3977–3980.

(45) Mó, O.; Riera, A. Excitation and charge exchange in He^++Na collisions. *Journal of Physics B: Atomic, Molecular and Optical Physics* **1988**, *21*, 119.

(46) Errea, L. F.; Méndez, L.; Mó, O.; Riera, A. Nonadiabatic ionic-covalent transitions. Exponential-linear model for the charge exchange and neutralization reactions $Na+H \rightleftharpoons Na^+ + H^-$. *The Journal of Chemical Physics* **1986**, *84*, 147–151.

(47) Bransden, B. H.; McDowell, M. H. C. *Charge Exchange and the Theory of Ion-Atom Collisions*; Oxford, Clarendon, 1992.

(48) Errea, L. F.; Harel, C.; Jouin, H.; Méndez, L.; Pons, B.; Riera, A. Common translation

factor method. *Journal of Physics B: Atomic, Molecular and Optical Physics* **1994**, *27*, 3603.

(49) Illescas, C.; Riera, A. Classical study of single-electron capture and ionization processes in $A^{q+} + (\mathrm{H}, \mathrm{H}_2)$ collisions. *Phys. Rev. A* **1999**, *60*, 4546–4560.

(50) Pacios, L. F.; Christiansen, P. A. Ab initio relativistic effective potentials with spin-orbit operators. I. Li through Ar. *The Journal of Chemical Physics* **1985**, *82*, 2664–2671.

(51) Schneiderman, S. B.; Russek, A. Velocity-Dependent Orbitals in Proton-On-Hydrogen-Atom Collisions. *Phys. Rev.* **1969**, *181*, 311–321.

(52) Piacentini, R.; Salin, A. Multistate molecular treatment of atomic collisions in the impact parameter approximation. II calculation of differential cross-sections from the transition amplitudes for the straight line case. *Computer Physics Communications* **1977**, *13*, 57 – 62.

(53) Gaussorgues, C.; Sech, C. L.; Masnou-Seeuws, F.; McCarroll, R.; Riera, A. Common trajectory methods for the calculation of differential cross sections for inelastic transitions in atom(ion)-atom collisions. II. Application to proton-hydrogen scattering. *Journal of Physics B: Atomic and Molecular Physics* **1975**, *8*, 253.

(54) Piacentini, R. D.; Salin, A. K-shell vacancy creation in asymmetric ion-atom collisions. *Journal of Physics B: Atomic and Molecular Physics* **1976**, *9*, 959.

(55) Winter, T. G.; Hatton, G. J.; Day, A. R.; Lane, N. F. Differential cross sections for electron transfer and elastic scattering in collisions between α particles and hydrogen atoms. *Phys. Rev. A* **1987**, *36*, 625–640.

(56) Errea, L. F.; López, A.; Méndez, L.; Riera, A. Elastic, inelastic and charge exchange differential cross sections in He^+ +H collisions. *Journal of Physics B: Atomic, Molecular and Optical Physics* **1992**, *25*, 811.

(57) Illescas, C.; Rabadán, I.; Riera, A. Illustration of the role of saddle-point and molecular-type ionization mechanisms in atomic collisions. *Phys. Rev. A* **1998**, *57*, 1809–1820.

(58) Muller, H. G. Numerical simulation of high-order above-threshold-ionization enhancement in argon. *Phys. Rev. A* **1999**, *60*, 1341–1350.

(59) Kramida, A.; Yu. Ralchenko,; Reader, J.; and NIST ASD Team, NIST Atomic Spectra Database (ver. 5.3), [Online]. Available: `http://physics.nist.gov/asd` [2017, October 2]. National Institute of Standards and Technology, Gaithersburg, MD., 2015.

(60) Labaigt, G.; Jorge, A.; Illescas, C.; Béroff, K.; Dubois, A.; Pons, B.; Chabot, M. Electron capture and ionization processes in high-velocity C_n^+, C-Ar and C_n^+, C-He collisions. *Journal of Physics B: Atomic, Molecular and Optical Physics* **2015**, *48*, 075201.

(61) Reinhold, C. O.; Falcón, C. A. Classical ionization and charge-transfer cross sections for H^++He and H^++Li^+ collisions with consideration of model interactions. *Phys. Rev. A* **1986**, *33*, 3859–3866.

(62) Talman, J. D. A program to compute variationally optimized effective atomic potentials. *Computer Physics Communications* **1989**, *54*, 85 – 94.

(63) Wehrman, L. A.; Ford, A. L.; Reading, J. F. Double ionization of helium by slow antiprotons. *J. Phys. B: At. Mol. Opt. Phys.* **1996**, *29*, 5831–5842.

(64) Illescas, C.; Errea, L. F.; Méndez, L.; Pons, B.; Rabadán, I.; Riera, A. Classical treatment of ion-H_2O collisions with a three-center model potential. *Phys. Rev. A* **2011**, *83*, 052704.

(65) Errea, L. F.; Illescas, C.; Méndez, L.; Rabadán, I. Ionization of water molecules by proton impact: Two nonperturbative studies of the electron-emission spectra. *Phys. Rev. A* **2013**, *87*, 032709.

(66) Kirchner, T.; Gulyás, L.; Lüdde, H. J.; Engel, E.; Dreizler, R. M. Influence of electronic exchange on single and multiple processes in collisions between bare ions and noble-gas atoms. *Phys. Rev. A* **1998**, *58*, 2063–2076.

(67) Davidson, E. R. MOTECC, Modern Techniques in Computational Chemistry. 1990.

(68) Castillo, J. F.; Errea, L. F.; Macías, A.; Méndez, L.; Riera, A. Ab initio calculation of nonadiabatic couplings using MELD. *The Journal of Chemical Physics* **1995**, *103*, 2113–2116.

(69) McLean, A. D.; Chandler, G. S. Contracted Gaussian basis sets for molecular calculations. I. Second row atoms, Z=11–18. *The Journal of Chemical Physics* **1980**, *72*, 5639–5648.

(70) Errea, L. F.; Guzmán, F.; Méndez, L.; Pons, B.; Riera, A. Ab initio calculation of charge-transfer and excitation cross sections in Li^++H(1s) collisions. *Phys. Rev. A* **2008**, *77*, 012706.

(71) Sidis, V. Some energy curves of ArH^+ and their use in the study of the scattering of H^+ by Ar. *Journal of Physics B: Atomic and Molecular Physics* **1972**, *5*, 1517.

(72) Errea, L. F.; Gorfinkiel, J. D.; Kryachko, E. S.; Macías, A.; Méndez, L.; Riera, A. Ab initio potential energy surfaces and nonadiabatic couplings involved in Be^{4+}+H_2 electron rearrangement. *The Journal of Chemical Physics* **1997**, *106*, 172–181.

(73) Errea, L. F.; Gorfinkiel, J. D.; Macías, A.; Méndez, L.; Riera, A. Ab initio calculation of charge transfer cross sections in C^{4+}+H_2 collisions. *Journal of Physics B: Atomic, Molecular and Optical Physics* **1999**, *32*, 1705.

(74) Errea, L. F.; Fernández, L.; Macías, A.; Méndez, L.; Rabadán, I.; Riera, A. Sign-consistent dynamical couplings between ab initio three-center wave functions. *The Journal of Chemical Physics* **2004**, *121*, 1663–1669.

(75) Stedeford, J. B. H.; Hasted, J. B. Further investigations of charge exchange and electron detachment - I. Ion energies 3 to 40 keV - II. Ion energies 100 to 4000 eV. *Proceedings of the Royal Society of London A: Mathematical, Physical and Engineering Sciences* **1955**, *227*, 466–486.

(76) Gordeev, Y. S.; Panov, M. N. Ionization and capture of electrons upon the collision of hydrogen ions with the atoms and molecules of gas. *Zh. Tekhn. Fiz.* **1964**, *34*, 857 [Sov. Phys. Tech. Phys. **9**, 656 (1964)].

(77) Johnson, L. K.; Gao, R. S.; Hakes, C. L.; Smith, K. A.; Stebbings, R. F. Direct and charge-transfer scattering of keV-energy H^+ and He^+ projectiles from rare-gas atoms to obtain small-angle absolute differential cross sections. *Phys. Rev. A* **1989**, *40*, 4920–4925.

(78) Heer, F. D.; Schutten, J.; Moustafa, H. Ionization and electron capture cross sections for protons incident on noble and diatomic gases between 10 and 140 keV. *Physica* **1966**, *32*, 1766 – 1792.

(79) Jorge, A.; Suárez, J.; Illescas, C.; Errea, L. F.; Méndez, L. Application of a grid numerical method to calculate state-selective cross sections for electron capture in Be^{4+}+H($1s$) collisions. *Phys. Rev. A* **2016**, *94*, 032707.

(80) Guzmán, F.; Errea, L. F.; Illescas, C.; Méndez, L.; Pons, B. Calculation of total cross sections and effective emission coefficients for B^{5+} collisions with ground-state and excited hydrogen. *Journal of Physics B: Atomic, Molecular and Optical Physics* **2010**, *43*, 144007.

(81) Jorge, A.; Errea, L. F.; Illescas, C.; Méndez, L. Calculation of ionization and total and partial charge exchange cross sections for collisions of C^{6+} and N^{7+} with H. *The European Physical Journal D* **2014**, *68*, 227.

(82) Rudd, M. E.; Kim, Y. K.; Madison, D. H.; Gallagher, J. W. Electron production in proton collisions: total cross sections. *Rev. Mod. Phys.* **1985**, *57*, 965–994.

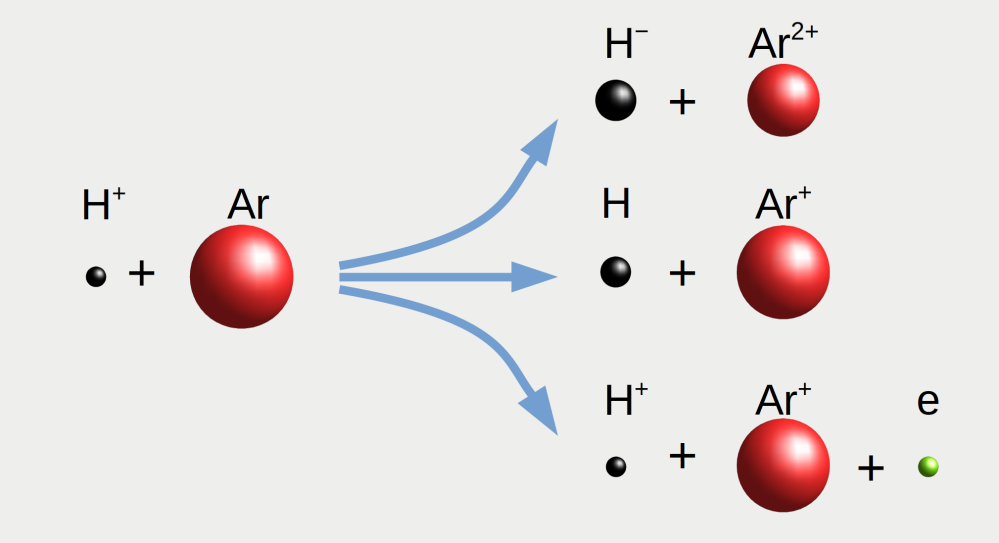
H+
Ar
H−
Ar2+
H
Ar+
H+
Ar+
e